Journal of Power Sources 195 (2010) 3416–3424

Contents lists available at ScienceDirect

Journal of Power Sources

journal homepage: www.elsevier.com/locate/jpowsour

Esterification as a diagnostic tool to predict proton conductivity affected by impurities on Nafion components for proton exchange membrane fuel cells

Kitiya Hongsirikarn, Xunhua Mo, James G. Goodwin*

Department of Chemical and Biomolecular Engineering, Clemson University, 128 Earle Hall, Clemson, SC 29634, USA

ARTICLE INFO

Article history:
Received 25 October 2009
Received in revised form 6 December 2009
Accepted 7 December 2009
Available online 16 December 2009

Keywords:
Conductivity prediction
Nafion
Ammonia
Na^+
Hydrocarbon
Fuel cell

ABSTRACT

Quantitative data of the effect of contaminants on individual components of a PEMFC is limited and difficult to acquire, especially for the ionomer in the catalyst layer. In this paper, we propose the use of an acid-catalysed reaction (esterification) as a method to quantitatively investigate the effect of contaminants on proton availability and conductivity of Nafion components, since proton sites in Nafion are also active as Brønsted acid sites for catalysis. It was found that at typical fuel cell conditions, ammonia adsorption decreased both conductivity and esterification activity of Nafion in a uniform manner. Because of the linear relationship between the number of proton/acid sites and both the conductivity and the esterification activity, a correlation between the two could be developed taking into account differences in the effect of humidity on the conductivity/activity of the poisoned Nafion. The methodology and correlation developed were also shown to predict accurately the effect of another impurity species (Na^+) on Nafion conductivity. The results demonstrate the application of esterification as a means to quantify the number of proton sites poisoned by adsorbing impurities, permitting the prediction of Nafion conductivity. This method would be applicable to both the membrane and ionomer in the catalyst layer.

1. Introduction

Fuel cells, especially proton exchange membrane fuel cells (PEMFCs), have received much attention for automotive, portable, and stationary applications because of many advantages, such as: low emission rate, high power density, low operating temperature, quick start up, quiet operation, and compactness [1–5]. Thus, fuel cells are a promising clean energy source for the future and have the potential to replace internal combustion engines. However, with current technology, the application of PEMFCs in transportation is limited due to high cost, insufficient Pt utilization, and particularly, lack of durability for contaminants in the hydrogen fuel and oxidant streams [1,6]. Unfortunately, significant levels of impurities including NH_3, CO_2, CO, H_2S, CH_4, and other organic compounds, that may poison and drastically degrade fuel cell performance can be inevitably contained in the hydrogen stream produced by hydrocarbon reforming, the most commonly used technology nowadays [7–10]. For instance, ammonia, one of the most detrimental impurities in the hydrogen stream for a PEMFC, can be present in a range up to 30–150 ppm [8,11,12]. Other impurities may also be present from a variety of sources [7,13–18].

In order to improve PEMFC performance and lifetime, fuller fundamental understanding of poisoning mechanisms must be obtained. The mechanisms of poisoning by such impurities as CO, CO_2, and H_2S on platinum or platinum alloy catalysts are fairly well understood [10,16–20]. However, research focusing on the specific impact of impurities and quantitative data about impurity coverage of the proton sites on individual electrolytes (membrane and catalyst ionomer layer for a PEMFC) are extremely limited. It has been found that under normal fuel cell operation in the absence of contaminants, proton transport limits fuel cell performance [21]. Thus, investigation of the effect of impurities on proton availability is extremely important.

Among commercial perfluorosulfonate ionomer (PFSI) electrolytes, Nafion shows the best performance in terms of durability, high proton conductance, and stability [22,23]. Results from previous work directly suggest that the ionic conductivity of a Nafion membrane is proportional to the concentration of free proton sites [24]. Thus, the conductivity of a Nafion membrane poisoned by ammonia or other impurities can be reasonably predicted by knowing the number of available proton sites, similar to the existing numerical simulation models that predict fuel cell performance in the presence of CO, CO_2, and H_2S because of their coverage of active sites on the Pt catalyst [16,25–27].

Although measurement of the number of free proton/acid sites occupied by ammonia or some of the other impurities can be analysed sometimes ex situ using ion-exchange with a cation solution

* Corresponding author. Tel.: +1 864 656 6614; fax: +1 864 656 0784.
E-mail address: jgoodwi@clemson.edu (J.G. Goodwin).

0378-7753/$ – see front matter © 2009 Elsevier B.V. All rights reserved.
doi:10.1016/j.jpowsour.2009.12.023

and employing an ion-selective electrode, it is not easy after incorporation in a membrane electrode assembly (MEA). Moreover, the amount of free proton sites in the presence of most other impurities and especially ones weakly adsorbed on the $-SO_3^-$–H^+ sites cannot be practically measured directly in situ or even ex situ for Nafion components (membrane and catalyst ionomer layer).

The focus of this study was to develop an easy and convenient technique to quantitatively determine the number of available proton sites of electrolytes under fuel cell operation conditions. The approach was to use a simple characteristic acid-catalysed reaction, the gas-phase esterification of acetic acid with methanol, on Nafion components as used in PEMFCs under conditions similar to fuel cell operation (typically 80 °C) to determine the surface coverage of impurities (e.g., ammonia) at the ppm level. The methanolysis reaction of acetic acid can take place at mild conditions (60–90 °C, 1 atm) and is thermodynamically favorable (equilibrium conversion ~96% at 80 °C) with 100% selectivity to methyl acetate. This reaction is possible to carry out using low concentrations of reactants. The results can be easily interpreted in terms of the number of proton/acid sites available because esterification, such as that of acetic acid with methanol (Eq. (1)), is a simple acid-catalysed reaction between nonsterically hindered alcohols and acids. The reaction occurs on a single reaction site in solid Brønsted acid catalysts like Nafion [28]:

$$CH_3OH + CH_3COOH \xrightarrow{H^+} CH_3COOCH_3 + H_2O \quad (1)$$

The organization of the article is as follows: (1) the conductivity, esterification activity and ammonium analyses of a Nafion membrane during exposure to ammonia over a wide range of conditions similar to those in a PEMFC (typically 80 °C) were obtained and compared; (2) the relationship between the availability of proton/acid sites on the Nafion membrane and the esterification activities under the similar conditions were determined and a model was proposed to predict conductivity based on esterification results; and (3) the accuracy of the model was then validated by comparing experimental results for conductivity for another contaminant (Na^+) with values of conductivity predicted by esterification.

2. Experimental

2.1. Materials

In order to obtain the fully H^+-form, Nafion membrane samples (N-211, DuPont), having a nominal thickness of 25.4 μm (50 g m^{-2}), were acidified by pretreating at 90 °C separately in aqueous solutions of: 3 wt.% H_2O_2 (Fisher Scientific), 0.5 M H_2SO_4 (Acros Organics), and deionized water for 1 h each. Then, the acidified membrane samples were rinsed and kept in deionized water at room temperature in the dark prior to the measurements.

Reagent-grade 1.0 M HCl (Fisher Scientific) and 99.99 wt.% NaCl (Fisher Scientific) were used to prepare the cationic forms (Na^+-form) of the Nafion®211 membrane (N-211). The H^+-form of N-211 was allowed to ion-exchange in aqueous solutions containing various metal cation compositions with total 0.1 M Cl^- for at least 10 days at room temperature under continuous shaking. The contaminant containing solutions were changed periodically during exchange equilibration. The conductivity measurements in deionized water of the exchanged membranes were performed over a 14-day period to ensure that the membranes reached equilibrium conductivity. Equilibrium was assumed when there was no conductivity difference of the membrane over a 2-day interval.

2.2. Material characterization

2.2.1. Elemental analysis

Elemental analyses (sulfur, nitrogen, and chlorine) of samples were conducted by Galbraith Laboratory in Knoxville, Tennessee (USA).

2.2.2. Ion-exchange capacity (IEC)

The concentrations of Brønsted acid sites on Nafion membranes (N-211, 5.5 cm × 1 cm, ~30 mg) were determined by titration. The membranes were ion-exchanged with 0.005 M NaOH (Acros Organics) at room temperature under constant shaking at 250 ppm for 2 days. Then, the membrane was removed and the aliquot was back-titrated with 0.005 M HCl (Acros Organics) using phenolphthalein as an indicator. The end point of titration was determined by pH meter at a pH of 7.

2.2.3. Cationic exchange capacity (CEC)

2.2.3.1. Membrane NH_4^+ content. Nafion membranes (N-211s) exposed to ammonia for a certain time in the conductivity chamber/esterification reactor were ion-exchanged with 0.05 M HCl (Acros Organics) at room temperature under constant shaking at 200 rpm for at least 7 days. Then, the sample was removed from the aliquot. The amount of ammonium ions in the exchange solution was analyzed using an ion-selective electrode (ammonia electrode 9512 Thermo Scientific and Orion 4 star pH benchtop meter).

2.2.3.2. Membrane Na^+ content. Following the conductivity or esterification measurements, the Na^+ composition in the membrane was determined by immersing the membrane in 0.005 M NaOH aqueous solutions at room temperature under constant shaking for 2 days, allowing Na^+ to neutralize the remaining acid sites. The membrane was then removed and the excess NaOH solution was back-titrated with 0.005 M HCl using phenolphthalein indicator. The end point was determined at a pH 7.

2.2.4. Thickness measurement

The only dimension change in the membrane during conductivity measurements was in the thickness. Thickness was measured immediately after conductivity measurement at five positions using a micrometer. The average of these measurements was used in the conductivity calculation.

2.3. Conductivity measurement

The conductivity of the N-211 membranes in a humidified gas phase was measured in a specially designed chamber by a two-probe ac impedance spectroscopic technique using a Gamry Potentiostat Reference 600. Since a membrane was fixed at both ends in a custom-made cell, change in the dimensions of the membrane during the experiment could cause stress and changes in membrane properties [29]. Thus, each membrane sample (5.5 cm × 1 cm) was initially equilibrated in a well-controlled environment overnight at a specific humidity under a flow of 130 sccm of He (UHP, National Specialty Gases). The humidity was obtained via a flash chamber. The water was introduced into the chamber and the flow rate was controlled by a syringe pump (Genie pump, Kent Scientific Corporation). A He stream was introduced passing through the separate heated chamber mixing with the water vapor. After that, the humidified He was flowed into the impedance measurement chamber where the relative humidity was monitored by a humidity and temperature transmitter (HMT 330, Vaisala).

The equilibrated "humidified" membrane was then sandwiched at both ends between two platinum foils and two custom-made polyetheretherketone (PEEK) sheets, and placed in the conductivity chamber (ID = 16 cm, H = 25 cm) at the specific temperature and

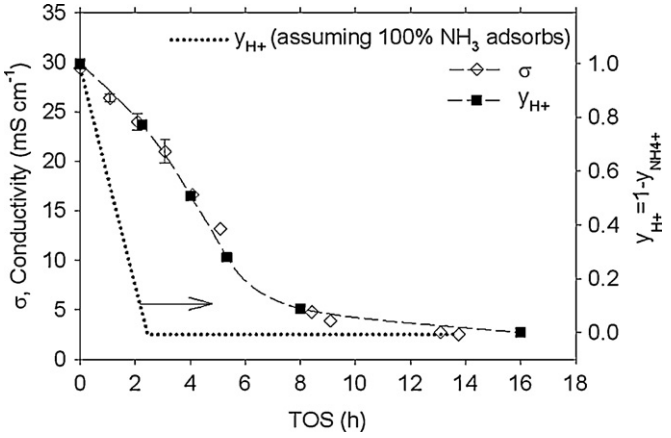

Fig. 1. The conductivity and NH_3 uptake of N-211 in the presence of 20 ppm NH_3 in flowing He at 50% RH and 80 °C as a function of TOS.

the same humidity as equilibration in a He atmosphere for 8 h. The conductivity was then measured until constant. After that, a given concentration of ammonia was introduced in a stream of He to the chamber, and the real time resistance measurement started. The conductivity was obtained from Eq. (2) in a frequency range of 100–1 kHz by extrapolating to get the real component on the complex impedance axis:

$$\sigma = \frac{L}{RA} \tag{2}$$

where σ is the proton conductivity ($S\,cm^{-1}$), L is the distance between the two platinum foils (2.5 cm), R is the resistance (Ω) of the membrane, A is the cross-sectional area of the membrane ($1\,cm \times t_{RH,T}$), and $t_{RH,T}$ is the thickness (cm) of the membrane depending on the relative humidity and temperature, respectively.

For a given study, the conductivity of a membrane exposed to ammonia in hydrogen flow was measured with time-on-stream (TOS) until a given time when the experiment was stopped. The membrane was then removed from the cell and the ammonium ion composition measured. Thus, figures such as Figs. 1 and 10(a) are a composite of successive runs.

The conductivity of pre-poisoned Na^+ Nafion membranes was measured after the membrane was pretreated at 30% RH and 80 °C for 8 h. Then, the humidity was raised by 15% RH steps from 30% RH to 100% RH and the conductivity was measured at each humidity equilibration.

2.4. Esterification measurement

Methanol (99.9 wt.%), acetic acid (99.7 wt.%), and methyl acetate (99 wt.%) were purchased from Fisher Scientific and used as supplied. Gas-phase esterification of methanol and acetic acid was carried out in a differential tubular reactor (ID = 0.7 cm) under various conditions. Prior to reaction, a sample of N-211 3 cm × 1 cm and 5.5 cm × 1 cm for 0–30% RH and 50–100% RH experiments, respectively was rolled up loosely with quartz wool (ChemGlass Inc.) separating the layers before being loaded in the middle of the reactior with a thermocouple close to the bed. The Nafion membrane was pretreated in situ in a 100 sccm H_2 at specific humidity, 80 °C, and 1 atm for 3 h. Afterwards, known quantities of acetic acid (HAc), methanol (MeOH), water vapor, and ammonia were introduced to the reactor. An equimolar ratio of MeOH:HAc was used in this study. The esterification was carried out at a given humidity, 80 °C, and 1 atm under a total flow rate of 100 sccm H_2. In order to avoid condensation inside the differential reactor and to minimize competitive adsorption of reactants with ammonia, the partial pressures of the reactants were kept low ($P_{MeOH} = P_{HAc} = 0.009$ atm). The rate of reaction is defined as the rate of methyl acetate formation (r_{MeOAc}). The concentrations of reactants (MeOH and HAc) and product (MeOAc) in the effluent stream were determined by a Varian CP-3380 GC equipped with an FID detector and a Varian CPWAX 52CB fused silica capillary column (60 m × 0.53 mm × 1 μm).

For the comparison of the conductivity and esterification activity of a Nafion membrane as a function of ammonium ion composition in the membrane ($y_{NH_4^+}$), the membrane was taken out of the reactor to determine ammonium uptake after a specified ammonia exposure time and ion-exchanged with 0.05 M HCl. Thus, Figs. 5 and 10(b) are a composite of successive duplicate runs for different periods of time. This was necessary since analysis of the ammonium ion concentration changes the membrane's properties.

The activity of esterification of pre-poisoned Na^+ Nafion membranes was investigated after the membrane was pretreated at 0% RH and 80 °C for 3 h. Then, the humidity was raised by 15% RH from 0% RH to 95% RH and the steady-state rate of methyl acetate (MeOAc) formation was measured at each humidity equilibration.

3. Results and discussion

3.1. Characterization

The ion-exchange capacity (IEC) of the fully acidified Nafion membrane (N-211) obtained from titration was $908 \pm 17\ \mu mol\ g^{-1}$, which is in agreement with sulfur analysis ($925\ \mu mol\ g^{-1}$).

3.2. Ionic conductivity of N-211

3.2.1. Effect of NH_3 concentration

The data points given in Fig. 1 show the changes in real time conductivity and in the amount of adsorbed ammonia (in the form of NH_4^+) in the Nafion membrane (N-211) at 50% RH, 80 °C, and 1 atm for 20 ppm NH_3 in 100 sccm H_2. The concentration of ammonium ions in the membrane ($C_{NH_4^+}$) was obtained via ion-exchange after the conductivity was investigated on the same membrane. However, since ammonia analysis is a destructive technique, each data point for y_{H^+} represents the proton composition in different N-211 membrane samples after exposure to 20 ppm NH_3 for a specified period of time. The amount of ammonia uptake ($y_{NH_4^+}$) and that of free proton sites (y_{H^+}) are defined as follows:

$$y_{NH_4^+} = \frac{C_{NH_4^+}}{[C_{H^+}]_0} \tag{3}$$

$$y_{NH_4^+} + y_{H^+} = 1 \tag{4}$$

where $y_{NH_4^+}$ and y_{H^+} are the fraction of sulfonic acid sites occupied by ammonium ions and protons, respectively; $C_{NH_4^+}$ is the concentration of ammonium ions interacting with the sulfonic groups in the Nafion membrane; and $[C_{H^+}]_0$ is the proton concentration (IEC) of the N-211 in the fully H^+-form, respectively.

In Fig. 1, the dotted line represents the ammonia uptake with time-on-stream (TOS) assuming 100% of ammonia introduced to the conductivity cell adsorbed on the membrane. It can be seen that the experimental data significantly deviates from the prediction because the flow characteristics inside an unstirred conductivity chamber (ID = 16 cm, H = 25 cm) are not efficient, allowing a lot of the ammonia to by-pass a membrane. For the actual data, as the amount of ammonia adsorption on the $-SO_3^-$–H^+ sites increases with time-on-stream (TOS), the conductivity decreases. In Fig. 2, the ionic conductivity of Nafion membrane can be seen to be linearly related to the concentration of free proton sites, (y_{H^+}), with the minimum conductivity representing that of the fully NH_4^+-form of the membrane. The rate of decrease in conductivity is determined by the flow rate of He, the efficiency of ammonia contacting the sites as a result of flow characteristics and diffusion, and the

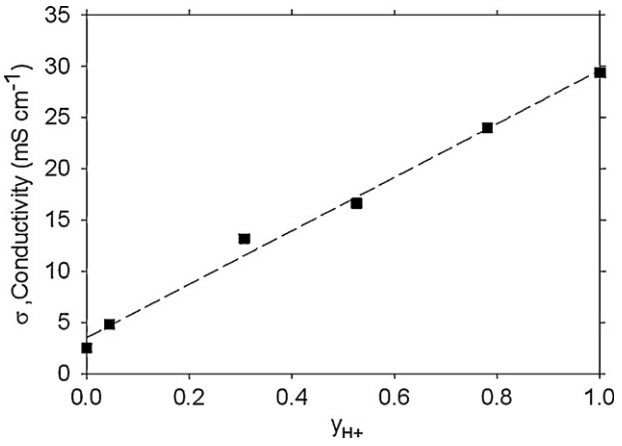

Fig. 2. Relationship of conductivity to proton fraction from Fig. 1.

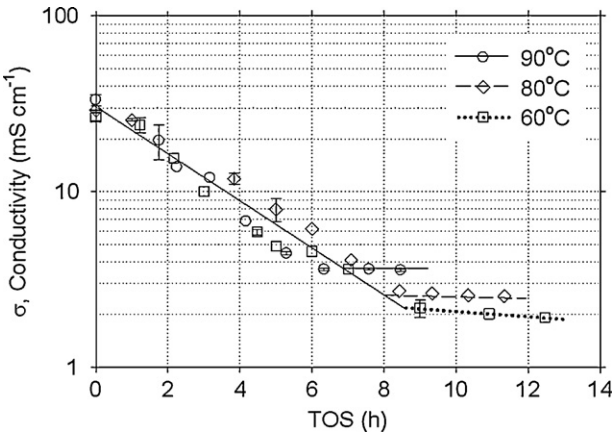

Fig. 3. The conductivity of N-211 in the presence of 20 ppm NH_3 in flowing He at 50% RH and various temperatures (60–90 °C).

concentration of ammonia since that concentration is so small compared to the number of sulfonic acid sites and the adsorption of ammonia is essentially irreversible. These results suggest that, in the presence of other contaminants that also adsorb on or block proton sites, the conductivity should be able to be predicted by knowing the concentration of proton sites.

3.2.2. Effect of humidity

In our previous work [24], the effect of the humidity on the conductivity of N-211 in the presence of 20 ppm NH_3 was studied and the results are summarized in Table 1. It was found that the kinetics of ammonia poisoning were slower and the steady-state conductivity was significantly increased with an increase in humidity. As discussed in that work, it is likely that water is beneficial to proton migration because of three reasons: (1) water competitively adsorbs on the $-SO_3^-$ groups and protects the sites from ammonia; (2) water weakens the acid strength of the sulfonic sites and increases water mobility in the ionic domain; and (3) water increases the hydrophilic region of the Nafion matrix resulting in the enhancement of the connectivity throughout the overall pore network.

3.2.3. Effect of temperature

In Fig. 3, the conductivities with TOS during ammonia exposure to the N-211 at various operating temperatures are illustrated. The initial and steady-state ionic conductivities slightly increased with an increase in operating temperature, consistent with results reported in the literature [30]. The rate of decrease in conductivity is not greatly affected by temperature since poisoning with ammonia is limited by the low ammonia concentration and the flow/diffusion characteristics (as stated at the end of Section 3.2.1), and not the rate of ammonia adsorption.

Table 1
Conductivity of N-211 in the H^+/NH_4^+-form with various proton compositions at 80 °C.

RH (%)	Conductivity[a] (mS cm^{-1})			
	y_{H^+} = 1.00[b] (H^+-form)	H^+/NH_4^+-form		
		y_{H^+} = 0.76[b]	y_{H^+} = 0.42[b]	y_{H^+} = 0.00[b] (NH_4^+-form)
30	10.4	8.44	4.64	0.23
40	15.5	–	–	–
50	29.5	23.4	14.7	3.9
60	40.0	–	–	–
70	61.2	–	–	–
80	90.3	64.4	44.2	19.3
90	129.6	92.0	65.2	32.2
100	182.5	148.9	105.3	51.4

[a] Conductivity; error = ±5%.
[b] NH_4^+ composition; error = ±7%.

3.3. Esterification activity of N-211

3.3.1. Effect of NH_3 concentration

Fig. 4 shows the cumulative effect of ammonia on esterification activity. As expected, irreversible ammonia adsorption onto the Brønsted acid sites of the Nafion membrane decreases the esterification activity in a similar fashion as it did the conductivity [24] under similar conditions. The only major difference was the time it took for maximum ammonia coverage due to the more efficient gas flow in the differential tubular reactor used for esterification (ID = 0.7 cm) compared to the unstirred conductivity chamber as mentioned in Section 3.2.1. It is clear that the number of free acid sites plays a significant role in both conductivity and acid-catalysed reaction. It has been reported that the number of free accessible acid sites is directly proportional to the rate of methyl acetate formation (r_{MeOAc}) [31].

Fig. 5 presents the decrease in esterification activity and accessible free acid sites (y_{H^+}) with TOS. The real time esterification activity was investigated on the same membrane, but the ammonia uptake was done on different samples under the exact same conditions. The dotted line shows the predicted esterification activity and ammonium ion composition assuming that all ammonia entering

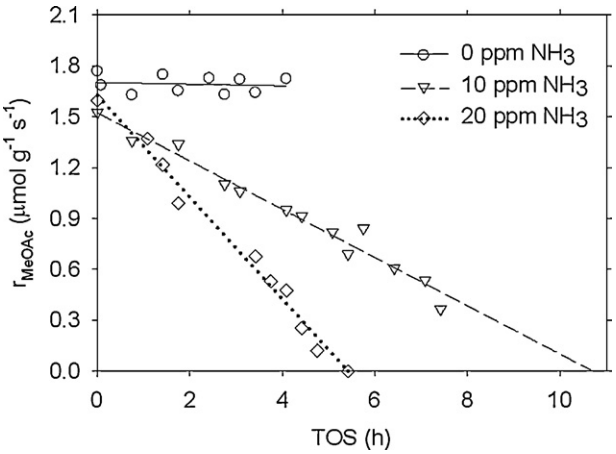

Fig. 4. Esterification activity of N-211 at different ammonia concentrations 50% RH and 80 °C in a H_2 atmosphere.

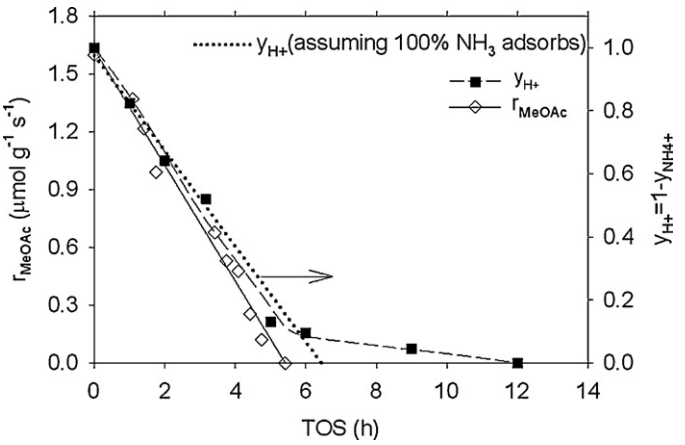

Fig. 5. Esterification activity and NH_3 uptake of N-211 in the presence of 20 ppm NH_3 in flowing H_2 at 50% RH and 80 °C as a function of TOS.

the reactor was absorbed by the membrane. It is evident the ammonia adsorption is much more efficient in the flow differential reactor than in the conductivity chamber. As can be seen in Fig. 5, the catalyst activity decreases slightly faster than the predicted value due to the effect of water poisoning (which will be discussed later) from the water produced as a by product of the reaction and the water in a feed stream. Also, the uptake of ammonia slightly differs from the estimated line because of a small amount of ammonia not being adsorbed during passage through the reactor and the difficulty to reach every site. The results replotted in Fig. 6 confirm the linear relationship between y_{H^+} and the esterification activity. The activity, however, is zero when there is <10% of the acid sites ($y_{H^+} \sim 0.1$) still remaining. There are three possible explanations for this phenomenon: (1) water molecules competitively adsorb with reactants (methanol and acetic acid) on the proton sites blocking them for reaction; (2) water vapor decreases the strength of the acid sites (acidity) by surrounding proton sites with fixed anionic charges [32]; and/or (3) water vapor favors the hydrolysis reaction (re-forming acetic acid from methyl acetate). In any case, the experimental data show that the threshold value for the reaction to occur under these conditions is $y_{H^+} \sim 0.1$ and the estimation of y_{H^+} using esterification below this threshold is not valid at these conditions.

It is evident from Figs. 2 and 6 that ammonia influences both conductivity and esterification activity in a similar manner under similar conditions.

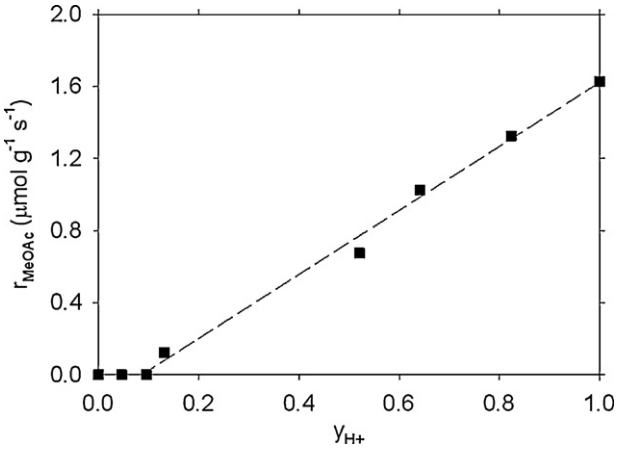

Fig. 6. Relationship of esterification activity to proton fraction from Fig. 5.

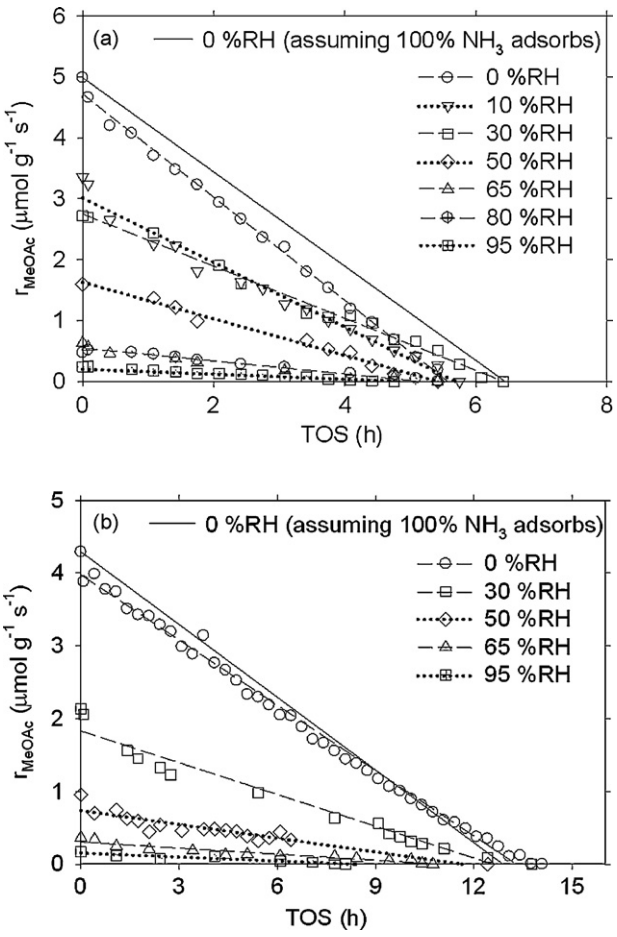

Fig. 7. Esterification activities of N-211 in the presence of 20 ppm NH_3 at 80 °C and 1 atm under a total flow of: (a) 100 sccm H_2 and (b) 50 sccm H_2. (The solid line represents the theoretical curve assuming that 100% of ammonia flowing through the reactor adsorbs onto the Brønsted acid sites.)

3.3.2. *Effect of humidity*

Fig. 7(a) and (b) show the effect of water vapor on the TOS activities of N-211 in the presence of 20 ppm NH_3 in H_2 at 50% RH, 80 °C, and 1 atm presence under total flows of 100 and 50 sccm. In Fig. 7(a) and (b), two different flow configurations were studied and compared in order to clarify how differences in flow characteristics can be compensated. The solid line shown in each figure represents the case for 0% RH where 100% of ammonia in the gas stream is adsorbed by the Nafion membrane. At all humidities, the actual time required to get full ammonium adsorption is the same as that at 0% RH (6.4 or 12.1 h depending on the flow rate), but the initial activity varied with humidity, suggesting that the competitive adsorption of water vapor with ammonia is minimal. Table 2 summarizes the esterification activity of pre-poisoned membranes at 80 °C and 1 atm with a total flow of 100 or 50 sccm H_2. It was found that under the same % RH, the activities under a total flow rate of 100 sccm were slightly higher than those of 50 sccm because the conversions in the former case (ca. 9% for 0% RH) were almost two times higher than the latter case (ca. 19% for 0% RH). Consequently, a larger concentration gradient of reactants occurred through the reactor for the lower flow rate.

Also, it is clear in Fig. 7(a) and (b) that the initial activities at both flow rates dramatically decreased as the humidity increased due to the three possible reasons mentioned in Section 3.3.1. These results are in good agreement with what has been reported in the literature [33–35]. At the same flow rate, although the initial activity varies with humidity, the time required for ammonia to poison all the

Table 2
Esterification activity of N-211 for various proton compositions at 80 °C in 20 ppm NH_3/H_2.[a].

RH (%)	r_{MeOAc} (μmol g^{-1} s^{-1})[b]				
	y_{H^+} = 1.00[c] (H^+-form)		y_{H^+} = 0.76[c]	y_{H^+} = 0.42[c]	y_{H^+} = 0.00[c] (NH_4^+-form)
	100 sccm	50 sccm	100 sccm	100 sccm	100 sccm
0	4.99	4.29	4.07	1.75	0
10	3.36	2.90	–	–	0
15	2.94	–	2.41	0.84	0
30	2.72	2.13	2.36	1.31	0
50	1.66	0.95	1.28	0.51	0
65	0.63	0.37	–	–	0
80	0.47	–	0.42	0.15	0
95	0.24	0.17	0.18	0.03	0

[a] At 1 atm with $P_{MeOH} = P_{HAc} = 0.009$ atm (balance H_2) with total flow of 100 or 50 sccm.
[b] Esterification activity; error = ±5%.
[c] NH_4^+ composition; error = ±7%.

active acid sites and the ammonium uptake at various humidities (30–100% RH, data shown later) was almost identical.

3.3.3. Effect of temperature

Fig. 8 illustrates the impact of temperature (60–90 °C) on the real time esterification activity in the presence of 20 ppm NH_3 at 50% RH and 1 atm. A slightly higher initial activity at higher temperature was observed, but the kinetics of activity decrease were similar because it was determined by the small concentration of ammonia in the gas flow. This observation is in good agreement with the conductivity data shown in Fig. 3.

3.4. Relationship between the conductivity and esterification activity of N-211

The results in Section 3.3 suggest the possibility for utilizing esterification as a quantitative technique to examine the number of available acid sites of the Nafion components during impurity exposure under various typical operation conditions of a fuel cell. Since both esterification activity and proton conductivity are affected directly by proton concentration, a possible correlation exists between these two processes with some corrections for the different effects of water vapor and for the flow characteristics on the two processes. The steady-state results of N-211 containing various compositions of H^+/cations (NH_4^+ or other contaminants) have to be adjusted before any comparison of the decrease in ionic conductivity and in esterification activity can be made. While water vapor favors proton transport, it poisons esterification. Thus, the conditions, that yield the best ionic conductivity and esterification activity, are at 100% RH and 0% RH, respectively. Thus, normalized conductivity ($\sigma_{Norm.}$) and esterification activity ($r_{MeOAc,Norm.}$) should be plotted against % relative humidity and 100% RH, respectively.

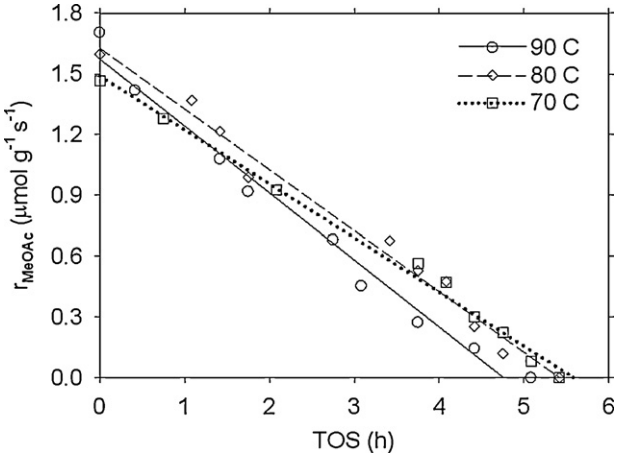

Fig. 8. Esterification activity of N-211 in the presence of 20 ppm NH_3 at 50% RH, 1 atm, and various temperatures (60–90 °C).

As shown in Tables 1 and 2, the steady-state conductivity of N-211 in the NH_4^+-form is not zero as is known, while the esterification activity for the NH_4^+-form is zero for every humidity. Therefore, the computation of $\sigma_{Norm.}$ and $r_{MeOAc,Norm.}$ should use the difference between the initial and final (steady state) of the conductivity and esterification activity and be normalized with that at the standard condition (100% RH for conductivity and 0% RH for esterification activity). The subtraction of the steady state from initial conductivity would not be required for impurities or contaminants that adsorb but produce no conductivity under fuel cell conditions; however, use of this general approach of subtraction should work in all cases.

The expressions for the normalized values for σ and r_{MeOAc} are as follows:

Conductivity:

$$\text{Normalized } \sigma(\sigma_{Norm.}) = \frac{(\sigma_{y_{H^+}=1} - \sigma_{y_{H^+}})_{RH,80\,^\circ C}}{(\sigma_{y_{H^+}=1} - \sigma_{y_{H^+}})_{100\%\ RH,80\,^\circ C}} \quad (5)$$

Esterification:

$$\text{Normalized } r_{MeOAc}(r_{MeOAc,Norm.}) = \frac{(r_{MeOAc,y_{H^+}=1} - r_{MeOAc,y_{H^+}})_{RH,80\,^\circ C}}{(r_{MeOAc,y_{H^+}=1} - r_{MeOAc,y_{H^+}})_{0\%\ RH,80\,^\circ C}} \quad (6)$$

where $\sigma_{y_{H^+}=1}$ and $\sigma_{y_{H^+}}$ are the conductivities of N-211 in the H^+-form and the mixed H^+/cations (NH_4^+ or other impurities) form, respectively; and $r_{MeOAc,y_{H^+}=1}$ and $r_{MeOAc,y_{H^+}}$ are the esterification activity of N-211 in the H^+-form and the mixed H^+/cations (NH_4^+ or other impurities) form, respectively.

Fig. 9 shows the comparison of the normalized ionic conductivities and esterification activities of Nafion membranes (N-211) under a wide range of humidities at 80 °C. The raw experimental data for this figure are given in Tables 1 and 2. After normalization, the $\sigma_{Norm.}$ (solid line) and $r_{MeOAc,Norm.}$ (dashed line) results essentially overlap. In Fig. 10(a) and (b), the numbers of available proton/acid sites (y_{H^+}) are linearly related to both the normalized ionic conductivity ($\sigma_{Norm.}$) and the normalized esterification activity ($r_{MeOAc,Norm.}$) under similar conditions at every humidity. This observation provides further justification for using esterification to probe the number of free proton sites at various conditions. However, Fig. 10(b) illustrates that the esterification activities at all humidities below ca. $y_{H^+} \sim 0.1$ are zero. Therefore, the $y_{H^+} \sim 0.1$ appears to be the threshold value for this reaction to occur, probably due to some acid sites not being readily exposed in the gas phase.

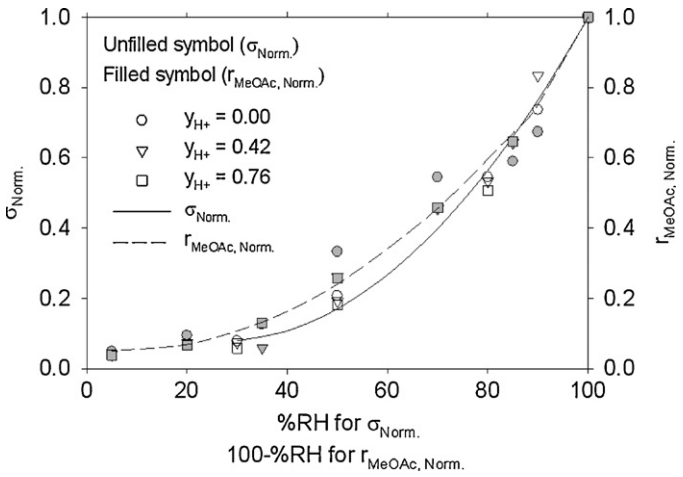

Fig. 9. Comparison of the conductivity and esterification activity of N-211 poisoned with NH_3 at 80 °C. ($\sigma_{Norm.}$ and $r_{MeOAc,Norm.}$ are normalized conductivity and normalized esterification activity obtained from Eqs. (5) and (6), respectively.)

3.5. Validity of esterification technique

The analysis in Section 3.4 suggests that esterification may be able to be used for any Nafion membrane contaminated with a substance interfering with its free proton sites to predict its conductivity under similar conditions based on Eqs. (5) and (6) and the relationship given by Fig. 9. To test the validity of this technique,

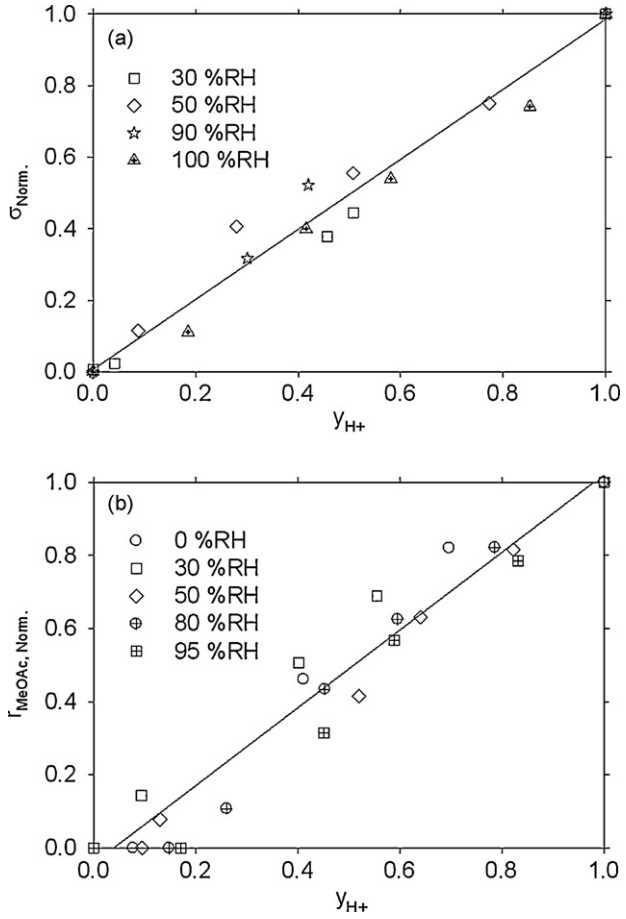

Fig. 10. The relationship of (a) normalized conductivity ($\sigma_{Norm.}$); and (b) normalized esterification activity ($r_{MeOAc,Norm.}$) of N-211 as a function of the fraction of proton sites at various humidities and 80 °C in the presence of NH_3.

Table 3
Steady-state esterification activity of N-211 in the H^+/Na^+-form at various proton compositions at 80 °C.[a].

RH (%)	r_{MeOAc} (μmol g^{-1} s^{-1})[b]			
	y_{H^+} = 1.00[c] (H^+-form)[d]	y_{H^+} = 0.82[c]	y_{H^+} = 0.41[c]	y_{H^+} = 0.00[c] (Na^+-form)
0	3.56	1.68	0.18	0
15	2.57	1.16	0.42	0
30	2.01	1.04	0.40	0
50	0.95	0.73	0.38	0
65	0.49	0.25	0.29	0
80	0.37	0.24	0.20	0
95	0.20	0.17	0.14	0

[a] At 1 atm with $P_{MeOH} = P_{HAc}$ = 0.009 atm (balance H_2) with total flow of 100 sccm.
[b] Esterification activity; error = ±5%.
[c] Na^+ composition; error = ±2%.
[d] N-211 in the H^+-form (ion-exchanged with 0.1 M HCl at room temperature at least 10 days).

the predicted steady-state conductivities of N-211 pre-poisoned with Na^+ were calculated from the normalized esterification activity ($r_{MeOAc,Norm.}$) and compared with experimental results. Table 3 summarizes the steady-state esterification activities at different humidities and 80 °C with different Na^+ concentrations in the membrane. It can be seen in Tables 2 and 3 that the esterification activities of N-211 in different binary-cationic forms (H^+/NH_4^+ and H^+/Na^+) are somewhat different under the same conditions, although these membranes contain similar proton compositions (y_{H^+}). This is because the acid strength of sulfonic acid sites is considerably influenced by the cationic property, distribution of foreign cation, and chlorine uptake in a Nafion membrane.

The co-existence of second counter ions in a membrane may significantly affect the acid strength of the sulfonic sites in the Nafion pore and channel. Previous studies have shown that cation contamination causes serious dehydration in a Nafion membrane [36,37]. The water uptakes (λ_{H_2O}) at 25 °C of a Nafion membrane (N-117) in the H^+-form, NH_4^+-form and Na^+-form are 21, 13.2, and 16.5 mol H_2O (mol SO_3^-)$^{-1}$, respectively [12,38]. The decrease of water in the Nafion structure leads to a compact structure which possibly affects the strength of acid sites in a pore and accessibility of reactants. Thus, it is not surprising that the activities for the acid-catalysed reaction (esterification) on N-211 in the H^+/Na^+-form would be somewhat different from those on the H^+/NH_4^+-form at the same conditions and y_{H^+}.

The distribution of the second cations, NH_4^+ or Na^+, in the membrane was non-uniform and uniform, respectively. For NH_4^+ poisoning, a fresh N-211 membrane was introduced to gas-phase ammonia; therefore, the membrane was poisoned from the outer to inner layers. For Na^+ contamination, on the other hand, the membrane was pre-poisoned by equilibrating in a standard solution containing a given H^+/Na^+ composition. Here, Na^+ ions in N-211 were distributed more uniformly in the Nafion matrix. Therefore, the presence of $-SO_3^-$–Na^+ in the vicinity of $-SO_3^-$–H^+ may interfere with the strength of the acid sites, which affects somewhat the linearity of the relationship between r_{MeOAc} and y_{H^+}.

Finally, previous study by Jones et al. [39] found that the amount of chloride uptake in a membrane increases with an increase in concentration of the exchange solution. The presence of these anions in the hydrophobic region could affect some properties of the Nafion membrane. In this study, the concentration of chloride in the standard solutions containing H^+ and Na^+ was fixed at 0.1 M Cl^-. The chlorine uptake of N-211 equilibrated in the H^+/Na^+ mixtures was ca. 5.3 μmol Cl g^{-1}, while the H^+/NH_4^+ membranes did not contain any chlorine. Therefore, it would be possible because of this that the esterification activity of N-211 in the H^+/NH_4^+ and H^+/Na^+-forms were slightly different, even though the membranes contained similar proton fractions (y_{H^+}). This is true even for y_{H^+} = 1 in the Na^+

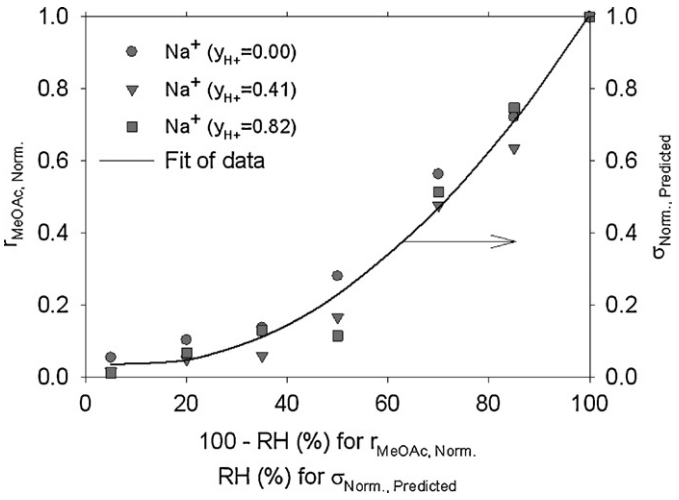

Fig. 11. A plot of normalized experimental esterification activities ($r_{MeOAc,Norm.}$) and predicted normalized conductivity ($\sigma_{Norm.,Predicted}$) for N-211 poisoned by Na^+.

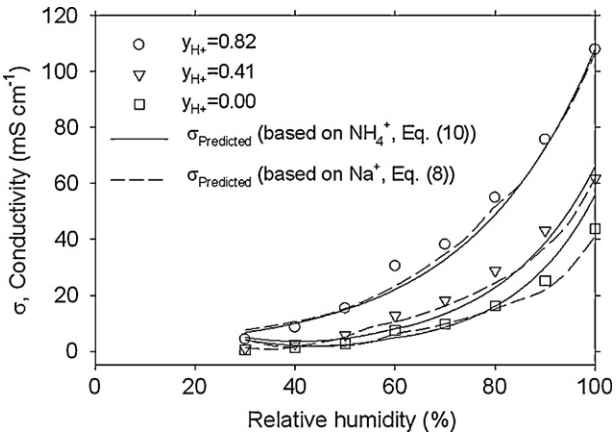

Fig. 12. Experimental and predicted ionic conductivities of N-211 in the H^+/Na^+-form at 80 °C.

study since it was treated in a solution containing HCl only so that its pretreatment would be similar to all other samples (except it would not have any Na^+).

The normalized esterification activities ($r_{MeOAc,Norm.}$) for the series of Na^+-contaminated membranes obtained from Eq. (6) using data in Table 3 are shown in Fig. 11. Based on results from the study of ammonia poisoning, we should be able to predict the normalized conductivity ($\sigma_{Norm.,Predicted}$) using the fit of the $r_{MeOAc,Norm.}$ data as shown in Fig. 11. To transform $\sigma_{Norm.,Predicted}$ to $\sigma_{y_{H^+}}$ for Na^+, we should use Eqs. (7) and (8). Unfortunately, the denominator term in Eq. (7) would not usually be known. Approximation of the denominator value from the pre-poisoned ammonium results might provide a reasonable estimation (Eq. (9)), because the properties of NH_4^+ and Na^+ ions are somewhat similar in terms of cation charge, cation size, mobility, interaction with bulk water and sulfonic sites, etc. [40–42]. Thus, expressing $\sigma_{Norm.,Predicted}$ by Eq. (9), we can solve for the desired predicted conductivity, $\sigma_{y_{H^+}}$, for Na^+, Eq. (10):

$$\sigma_{Norm.,Predicted} = \frac{[(\sigma_{y_{H^+}=1} - \sigma_{y_{H^+}})_{RH,80\,^\circ C}]_{Na^+}}{[(\sigma_{y_{H^+}=1} - \sigma_{y_{H^+}})_{100\%\ RH,80^\circ C}]_{Na^+}} \quad (7)$$

$$[(\sigma_{y_{H^+}})_{RH,80\,^\circ C}]_{Na^+} = [(\sigma_{y_{H^+}=1})_{RH,\ 80\,^\circ C}]_{Na^+} - \sigma_{Norm.,Predicted}[(\sigma_{y_{H^+}=1} - \sigma_{y_{H^+}})_{100\%\ RH,80^\circ C}]_{Na^+} \quad (8)$$

$$\sigma_{Norm.,Predited} \approx \frac{[(\sigma_{y_{H^+}=1} - \sigma_{y_{H^+}})_{RH,\ 80\,^\circ C}]_{Na^+}}{[(\sigma_{y_{H^+}=1} - \sigma_{y_{H^+}})_{100\%\ RH,80^\circ C}]_{NH_4^+}} \quad (9)$$

$$[(\sigma_{y_{H^+}})_{RH,80\,^\circ C}]_{Na^+} \approx [(\sigma_{y_{H^+}=1})_{RH,80\,^\circ C}]_{Na^+} - \sigma_{Norm.,Predicted}[(\sigma_{y_{H^+}=1} - \sigma_{y_{H^+}})_{100\%\ RH,80^\circ C}]_{NH_4^+} \quad (10)$$

In Fig. 12, the solid lines show the predicted conductivities of the N-211 membrane with different Na^+ concentrations and at different % RH using the experimental conductivities at 100% RH of N-211 pre-poisoned with NH_4^+ having $y_{H^+} = 0.00$, 0.41, 0.82, and 1.00 (56.3, 67.1, 110.9, and 161.5 mS cm^{-1}, respectively [24]). The reason why we did not use the conductivity results provided in Table 1 is due to the difference in impurity distribution of contaminated membranes. As mentioned in Section 3.2, Table 1 lists the conductivity of a membrane exposed to gas-phase ammonia. The results used from Ref. [24] were for NH_4^+ contaminated membrane prepared using an aqueous solution, similar to the case for Na^+.

Actual conductivity measurements were made for the Na^+ contaminated N-211 membranes at various % RHs and the results are given in Table 4. These data are also plotted in Fig. 12 for comparison to the predicted values. As one can see, there is a very good fit of the predicted values to the experimental results.

In order to evaluate the impact of estimating $[(\sigma_{y_{H^+}=1} - \sigma_{y_{H^+}})_{100\%\ RH,80^\circ C}]_{Na^+}$ using the values for NH_4^+ poisoned N-211 instead, results from Table 4 were used to calculate this term. The dashed lines in Fig. 12 represent the predicted conductivities using Eq. (8) based on Na^+ data at 100% RH. It can be seen that the predictions based on either NH_4^+ or Na^+ results at 100% RH are practically identical. The biggest difference was for $y_{H^+} = 0$, i.e., for the fully Na^+ exchanged membrane, and % RH > 80%. This may be possibly due to the difference in the water–water and cationic–water interactions [43]. The hydrogen bonds of water molecules in the vicinity of NH_4^+ and Na^+ ions may be different at high cationic content and high water concentration in a Nafion structure. Also, the intermolecular force of the H-bond between water molecules and NH_4^+ ions is different from that of the dipole–dipole force between water molecules and Na^+ ions.

The agreement of prediction with experimental data shown in this study confirms that after normalization, the relative effect of foreign impurities on both ionic conductance and esterification is almost identical. On the other hand, impurities, that we have found to not affect ionic conductance of a Nafion membrane (e.g., CO_2,

Table 4
Experimentally measured steady-state conductivity of N-211 in the H^+/Na^+-form with various proton compositions at 80 °C.

RH (%)	Conductivity (mS cm^{-1})[a]			
	$y_{H^+} = 1.00$[b] (H^+-form)[c]	H^+/Na^+-form		
		$y_{H^+} = 0.82$[c]	$y_{H^+} = 0.41$[c]	$y_{H^+} = 0.00$[c] (Na^+-form)
30	10.6	4.24	1.03	0.39
40	15.4	8.51	2.71	1.16
50	29.4	15.3	5.79	2.70
60	38.2	30.5	12.7	7.40
70	56.2	38.2	18.3	9.72
80	78.6	59.4	28.8	16.2
90	105.3	75.7	43.1	25.3
100	161.5	107.9	61.8	43.8

[a] Conductivity; error = ±5%.
[b] N-211 in the H^+-form (ion-exchanged with 0.1 M HCl at room temperature at least 10 days).
[c] Na^+ composition; error = ±2%.

CO, HCOOH, C_2H_4, CH_3CHO, C_4H_8O (tetrahydrofuran), etc.), also do not affect esterification activity (data not presented here). This is because they do not adsorb on the anionic sulfonic charges and/or interfere with the strength of acid/proton sites.

This study validates the use of esterification as a powerful analysing technique to quantitatively analyse the number of active proton sites (directly related to esterification activity in the absence of mass transport limitations) and to predict ionic conductivity of the membrane over a wide range of humidity under operational fuel cell conditions. The correlation has been shown to work for monovalent cations (NH_4^+ and Na^+). The applicability of this correlation to polyvalent cationic ions (e.g., Ca^{2+}, Mg^{2+}, Fe^{3+}, Cr^{3+}) will be the subject of future research.

It is important to note that the conductivity of a Nafion membrane in this study was measured in the in-plane direction because this method provided many benefits in terms of high reproducibility and accuracy, ease of operation, and low noise. However, the conductivity in the direction of thickness may be somewhat different than that in the lateral direction. It has been found that the conductivity of a Nafion 117 membrane can be anisotropic [44]. Nevertheless, the conductivity prediction (Eq. (5)) should be valid in both cases. In this work, we successfully predicted the in-plane conductivity of Na^+-poisoned membranes using Eq. (5) and experimental data given in Table 4. Likewise, conductivity in the thickness direction should also be able to be estimated by the same methodology, but using conductivity results in the direction of thickness instead for the correlation.

4. Conclusions

In this study, the effect of impurity poisoning (such as by ammonia) on the proton availability of Nafion membranes at conditions typical of a fuel cell was investigated. The influence of ammonia on a Nafion membrane (N-211) was examined for the first time by making use of conductivity measurements, ammonia uptakes, and an acid-catalyzed reaction for Brønsted acid sites (esterification). It was found that in the presence of ammonia, the conductivity N-211 decreases at 80 °C and all humidities in proportion to an increase in ammonia adsorption onto proton sites. This observation suggested that the ionic conductivity of Nafion membranes should be able to be plausibly predicted by knowing the proton compositions in them. This work proposes a convenient alternative technique to numerically investigate the number of acid sites during impurity exposure using a simple esterification reaction catalysed by the proton sites. The ammonia analyses confirm a linear correlation both between number of proton/acid sites ($-SO_3^-–H^+$) and both the conductivity and esterification catalytic activity under various conditions (0–95% RH, 1 atm, and 80 °C). Despite some dissimilarities between these two reactions, for example, the mechanism (ionic transport and acid-catalysed reaction), effect of water vapor (beneficial to conductivity and detrimental to esterification activity), and flow characteristics (non-ideal flow in an unstirred conductivity chamber and ideal flow in a differential esterification reactor), the normalization of the difference between the initial (or non-poisoned) and steady-state (or poisoned) conductivity and esterification activity allows us to establish a relationship between these two processes.

In this work, it was found that for a gas-phase ammonia poisoned membrane, the normalized conductivity ($\sigma_{Norm.}$) and normalized esterification activity ($r_{MeOAc,Norm.}$) under % RH and 100% RH, respectively were similar. We were then able to use esterification activity to predict the conductivity of a membrane contaminated with Na^+ at various ionic contents under practical fuel cell conditions. It was found that the predicted conductivity was in good agreement with the experimental conductivity at all proton compositions (y_{H^+}) and humidity ranges. These results justify the use of esterification as a diagnostic tool to quantitatively investigate the proton availability and predict the ionic conductivity of Nafion components in the presence of other contaminants at various conditions. This should be especially useful for predicting ionic conductivity of the ionomer in the catalyst layer – something that is difficult/impossible to directly measure. Such predictions of conductivity for both the ionomer and membrane should be useful for future fuel cell simulation work.

Acknowledgements

This work was financially supported by the U.S. Department of Energy (award no. DE-FG36-07GO17011). KH is very grateful to Michael E. DeWitt, Jr., Dr. Kaewta Suwannakarn, and Jia Gao for several discussions and comments about data analysis.

References

[1] Z.T. Xia, Q.P. Wang, M. Eikerling, Z.S. Liu, Can. J. Chem. 86 (7) (2008) 657.
[2] U. Beuscher, S.J.C. Cleghorn, W.B. Johnson, Int. J. Energy Res. 29 (12) (2005) 1103.
[3] Z.D. Wei, H.B. Ran, X.A. Liu, Y. Liu, C.X. Sun, S.H. Chan, P.K. Shen, Electrochim. Acta 51 (15) (2006) 3091.
[4] A. Collier, H.J. Wang, X.Z. Yuan, J.J. Zhang, D.P. Wilkinson, Int. J. Hydrogen Energy 31 (13) (2006) 1838.
[5] M.S. Mikkola, T. Rockward, F.A. Uribe, B.S. Pivovar, Fuel Cells 7 (2) (2007) 153.
[6] P.P. Kundu, A. Pal, Rev. Chem. Eng. 22 (3) (2006) 125.
[7] C.G. Farrell, C.L. Gardner, M. Ternan, J. Power Sources 171 (2) (2007) 282.
[8] F.A. Uribe, S. Gottesfeld, T.A. Zawodzinski, J. Electrochem. Soc. 149 (3) (2002) A293.
[9] L. Barelli, G. Bidini, F. Gallorini, S. Servili, Energy 33 (4) (2008) 554.
[10] X. Cheng, Z. Shi, N. Glass, L. Zhang, J.J. Zhang, D.T. Song, Z.S. Liu, H.J. Wang, J. Shen, J. Power Sources 165 (2) (2007) 739.
[11] R. Halseid, P.J.S. Vie, R. Tunold, J. Power Sources 154 (2) (2006) 343.
[12] R. Halseid, P.J.S. Vie, R. Tunold, J. Electrochem. Soc. 151 (3) (2004) A381.
[13] T. Okada, N. Nakamura, M. Yuasa, I. Sekine, J. Electrochem. Soc. 144 (8) (1997) 2744.
[14] T. Okada, Y. Ayato, M. Yuasa, I. Sekine, J. Phys. Chem. B 103 (17) (1999) 3315.
[15] M.J. Kelly, G. Fafilek, J.O. Besenhard, H. Kronberger, G.E. Nauer, J. Power Sources 145 (2) (2005) 249.
[16] G.J.M. Janssen, J. Power Sources 136 (1) (2004) 45.
[17] J.C. Davies, G. Tsotridis, J. Phys. Chem. C 112 (9) (2008) 3392.
[18] W.Y. Shi, B.L. Yi, M. Hou, Z.G. Shao, Int. J. Hydrogen Energy 32 (17) (2007) 4412.
[19] R.C. Urian, A.F. Gulla, S. Mukerjee, J. Electroanal. Chem. 554 (2003) 307.
[20] A.A. Shah, P.C. Sui, G.S. Kim, S. Ye, J. Power Sources 166 (1) (2007) 1.
[21] A. Katsaounis, S.P. Balomenou, D. Tsiplakides, M. Tsampas, C.G. Vayenas, Electrochim. Acta 50 (25–26) (2005) 5132.
[22] F.M. Collette, C. Lorentz, G. Gebel, F. Thominette, J. Membr. Sci. 330 (1–2) (2009) 21.
[23] T. Li, A. Wlaschin, P.B. Balbuena, Ind. Eng. Chem. Res. 40 (22) (2001) 4789.
[24] K. Hongsirikarn, J.G. Goodwin Jr., S. Greenway, S. Creager, J. Power Sources 195 (1) (2010) 30.
[25] A.A. Shah, F.C. Walsh, J. Power Sources 185 (1) (2008) 287.
[26] P. Rama, R. Chen, R. Thring, Proc. Inst. Mech. Eng. A: J. Power Energy 220 (A6) (2006) 535.
[27] M. Minutillo, A. Perna, Int. J. Energy Res. 32 (14) (2008) 1297.
[28] Y.J. Liu, E. Lotero, J.G. Goodwin Jr., J. Catal. 242 (2) (2006) 278.
[29] D. Liu, M.A. Hickner, S.W. Case, J.J. Lesko, J. Mater. F: Eng. Technol.-Trans. ASME 128 (4) (2006) 503.
[30] J.H Jang, H.C. Chiu, W.M. Yan, W.L. Sun, J. Power Sources 180 (1) (2008) 476.
[31] K. Suwannakarn, E. Lotero, J.G. Goodwin Jr., Catal. Lett. 114 (3–4) (2007) 122.
[32] C.W. Hu, M. Hashimoto, T. Okuhara, M. Misono, J. Catal. 143 (2) (1993) 437.
[33] Y.J. Liu, E. Lotero, J.G. Goodwin Jr., J. Mol. Catal. A: Chem. 245 (1–2) (2006) 132.
[34] R. Aafaqi, A.R. Mohamed, S. Bhatia, J. Chem. Technol. Biotechnol. 79 (10) (2004) 1127.
[35] D. Kusdiana, S. Saka, Bioresour. Technol. 91 (3) (2004) 289.
[36] T. Okada, H. Satou, M. Okuno, M. Yuasa, J. Phys. Chem. B 106 (6) (2002) 1267.
[37] T. Okada, S. Moller-Holst, O. Gorseth, S. Kjelstrup, J. Electroanal. Chem. 442 (1–2) (1998) 137.
[38] T. Okada, G. Xie, O. Gorseth, S. Kjelstrup, N. Nakamura, T. Arimura, Electrochim. Acta 43 (24) (1998) 3741.
[39] P.N.P. Leslie Jones, Hao Tang, J. Membr. Sci. 162 (1–2) (1999) 135.
[40] J.C. Slater, J. Chem. Phys. 41 (10) (1964) 3199.
[41] M. Doyle, M.E. Lewittes, M.G. Roelofs, S.A. Perusich, R.E. Lowrey, J. Membr. Sci. 184 (2) (2001) 257.
[42] A.A. Khan, W.H. Baur, Acta Cryst. B 28 (March) (1972) 683.
[43] F. Floris, M. Persico, A. Tani, J. Tomasi, Chem. Phys. 195 (1–3) (1995) 207.
[44] M. Shuhua, S. Zyun, T. Hirokazu, J. Electrochem. Soc. 153 (12) (2006) A2274.